Ab initio study of linear and nonlinear optical properties of mixed tellurite–chalcogenide glasses

2010 J. Phys.: Condens. Matter 22 165903

(http://iopscience.iop.org/0953-8984/22/16/165903)

J. Phys.: Condens. Matter **22** (2010) 165903 (8pp) doi:10.1088/0953-8984/22/16/165903

Ab initio study of linear and nonlinear optical properties of mixed tellurite–chalcogenide glasses

Zhian Jin, Ivan Biaggio and Jean Toulouse

Department of Physics and Center for Optical Technologies, Lehigh University, Bethlehem, PA 18015, USA

E-mail: zhj204@lehigh.edu

Received 21 December 2009, in final form 8 March 2010
Published 6 April 2010
Online at stacks.iop.org/JPhysCM/22/165903

Abstract

We discuss the potential functionalities of a mixed tellurite–chalcogenide glass where alternate oxygen atoms in a TeO_2 vitreous network are substituted with either sulfur or selenium atoms. We calculate the microscopic linear and nonlinear polarizabilities of chains with a finite number (n) of TeOX (X = S or Se) units from *ab initio* quantum chemistry computations and apply rotational averaging to the results. We find that the rotationally averaged linear polarizability, α_{av}, increases linearly with the number of units, while the second hyper-polarizability, γ_{av}, grows as a power law with an exponent that changes from 1.2 to 1.9 and 2.4 when going from pure tellurite to S substitution and Se substitution, respectively. We then estimate the density of the resulting glass and local field corrections to obtain the macroscopic linear and nonlinear susceptibilities for a glass made from chains of $n = 5$. We find that the extra Te–S (or Te–Se) bonds in the mixed tellurite–chalcogenide system enhance the linear refractive index n_0 and the third-order susceptibility $\chi^{(3)}$ by factors of ∼1.3 (or 1.4) and ∼8 (or 14), respectively, over the base tellurite glasses (X = O).

(Some figures in this article are in colour only in the electronic version)

1. Introduction

Nonlinear optical materials with high third-order nonlinearity and good chemical stability at room temperature play an important role in realizing such applications as all-optical switching [1] and supercontinuum light sources [2]. Both tellurite and chalcogenide non-silica glasses containing one or more element from group VI of the periodic table (O, S, Se and Te) are considered good material candidates, exhibiting third-order nonlinear optical susceptibilities $\chi^{(3)}(-\omega; \omega, \omega, -\omega)$ with typical values, respectively, ∼50 times and ∼1000 times larger than that of fused silica [3, 4]. The remarkable nonlinearity of the chalcogenide glasses is due to their more polarizable covalent bonds and lower energy gap. Unfortunately, the chemical instability and photosensitivity of chalcogenide glasses in air and at room temperature imposes limits on their reliability for some practical applications. Tellurite glasses (TeO_2) have also received attention as new oxide glasses because they are quite stable chemically and structurally, even though they exhibit lower values of $\chi^{(3)}$ than chalcogenide glasses. It is therefore of great interest to try and combine in a new glass the positive features from both tellurites and chalcogenides, but before starting to work on the synthesis of such a new material it is important to investigate its potential functionalities quantitatively. The starting idea of the present work is therefore to quantitatively estimate the effect on the optical and nonlinear optical properties of the glass of substituting chalcogen elements for oxygen ions, which should locally reduce the excited state energy, create a more polarizable chalcogen bond, and favor a slight delocalization of the electrons over several bonds. With this objective in mind, we have performed an *ab initio* calculation of the structure and of the linear and third-order optical polarizabilities of pure TeO_2 molecular chains present in the glass network, and how they are modified by substitution of sulfur or selenium for oxygen in molecular chains. The choice of the particular molecular chain is described and justified below. We also use the microscopic polarizabilities to estimate the resulting

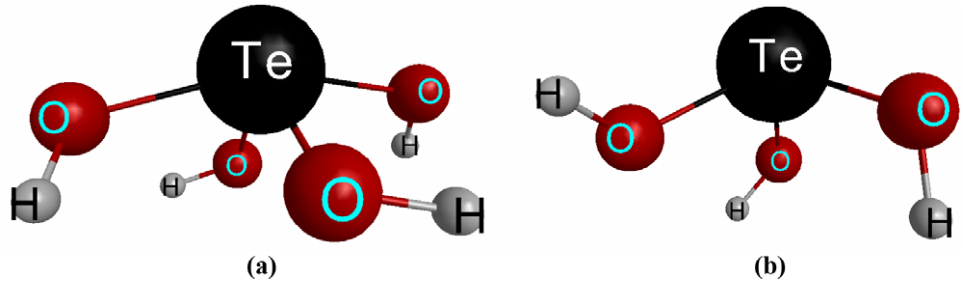

Figure 1. Two basic molecular structures of tellurite glasses, (a) TeO_4 and (b) TeO_3^+, are simulated in GAMESS [8] and plotted in MacMolPlt [35].

macroscopic linear and nonlinear susceptibilities of the pure tellurite glass and how they change when adding S and Se in this way. Such a glass would be expected to have higher nonlinear optical susceptibilities, while preserving the good chemical stability and low photosensitivity of an oxide glass.

Engineering Te–X (X = S or Se) bonds within an oxidized tellurium environment is challenging, since commonly known oxides containing tellurium and other chalcogen element(s) tend to form chalcogen–oxygen bonds under conventional fabrication processes [5, 6]. Nevertheless, a practical way of effectively synthesizing the ternary compounds with both Te–O and Te–X (X = S or Se) bonds is under development in our laboratory and we have recently succeeded in synthesizing a TeO_2–5% ZnS glass [7]. In parallel, the main purpose of this paper is to study theoretically the possible enhancement of the linear and nonlinear susceptibilities that could be obtained from the S or Se substitution. Such modeling can provide useful guidance in the search for a suitable mixed glass. In the following, we report the results of an investigation of the microscopic linear polarizability and the third-order polarizability (second hyper-polarizability) on a molecular scale, using a quantum chemistry computation package, General Atomic and Molecular Electronic Structure System (GAMESS) [8], and the *ab initio* theoretical approach of linear combination of atomic orbitals–molecular orbitals (LCAO-MO) [9–12]. The computed microscopic quantities are then used together with the density of the resulting glass and rotational averaging of the polarizability tensors to estimate the linear and nonlinear optical susceptibilities ($\chi^{(1)}$ and $\chi^{(3)}$) of the bulk material and their mutual relationship, including a comparison with the trend predicted by the equivalent of Miller's rule for third-order nonlinear optics ($\chi^{(3)}/[\chi^{(1)}]^4 \sim$ constant) [13].

Since it has been suggested that the length of the molecular clusters within TeO_2-based glasses has an important effect on the optical nonlinearity [14, 15], we calculate the linear and nonlinear optical performance of a tellurite–chalcogenide mixed glass for chains of $^{H-O}{}_{H}{>}Te{<}^{O}{}_{X}{>}Te{<}^{X}{}_{O}\cdots{}^{O}{}_{X}{>}Te{<}^{X}{}_{O}{>}Te{<}^{H}{}_{O-H}$ (X = S or Se) of different lengths, i.e. a variable number (n) of basic TeOX units embedded in the TeO_2 network. In order to estimate an upper limit for the coefficients that can be obtained in such a mixed glass, we chose a ∼50% chalcogen substitution in our study, i.e. every other oxygen atom being replaced by a chalcogen atom.

2. Molecular clusters

The basic structural units of tellurite glasses (TeO_2-based glasses) and their properties have been widely studied both experimentally and theoretically [3, 16–20]. Unlike silicate glasses having stable SiO_4 tetrahedra that are not easily modified by additional dopants, tellurite glasses can form various molecular polyhedra of TeO_x (x = 3–6) depending on the type and the number of modifier atoms introduced and material fabrication processes [16]. Among them, the TeO_4 trigonal bipyramid and the TeO_3^+ trigonal pyramid polyhedra shown in figure 1 are the most commonly observed basic structural units in the tellurite vitreous network. The corner-sharing TeO_4, with two longer Te–O bonds (axial bonds) and two shorter ones (equatorial bonds), either remains as a single cluster or connects to others as $^{O}{}_{O}{>}Te{<}^{O}{}_{O}{>}Te{<}^{O}{}_{O}$, to maintain the bridging function of the oxygen ion that forms the basic TeO_2 network. In practice, pure TeO_2 does not form a glass but crystallizes in one of three forms, α-TeO_2 [21], β-TeO_2 [22] or γ-TeO_2 [18] with variable bond lengths due to different arrangements of the corner-sharing distorted tetrahedra TeO_4 [20]. In order to form a tellurite glass, modifiers such as Na or Zn must be added [16]. One of the most studied tellurite compositions for optical applications has been $75TeO_2$–$20ZnO$–$5Na_2O$. Other compositions have also been studied. In particular, we and other groups have shown that the introduction of Zn leads to the formation of new molecular units, which can be concatenated to form chains such as Te_2O_5, Te_3O_8 and Te_3O_{11}, in which Zn charge compensates for non-bridging oxygens in the chain [23–25]. It is worth noting that there in fact exists a crystal with composition $Zn_2Te_3O_8$. A three-dimensional chainlike structure made up of these new molecular units concatenated in chains therefore appears to be an essential structural feature of mixed tellurite glasses [19, 20]. Taking advantage of this characteristic feature of tellurite glasses, it is interesting to investigate the possibility of substituting chalcogen elements for oxygen within these units and form chalcogen molecular units within the oxide glass.

Among several molecular structures $(TeO_2)_n$ that have been simulated in *ab initio* calculations [14], the chain-like structure promises to possess large electron polarization. This structure has therefore received more attention [15]. The basic chainlike connections of the localized molecular network in tellurite glasses have the form

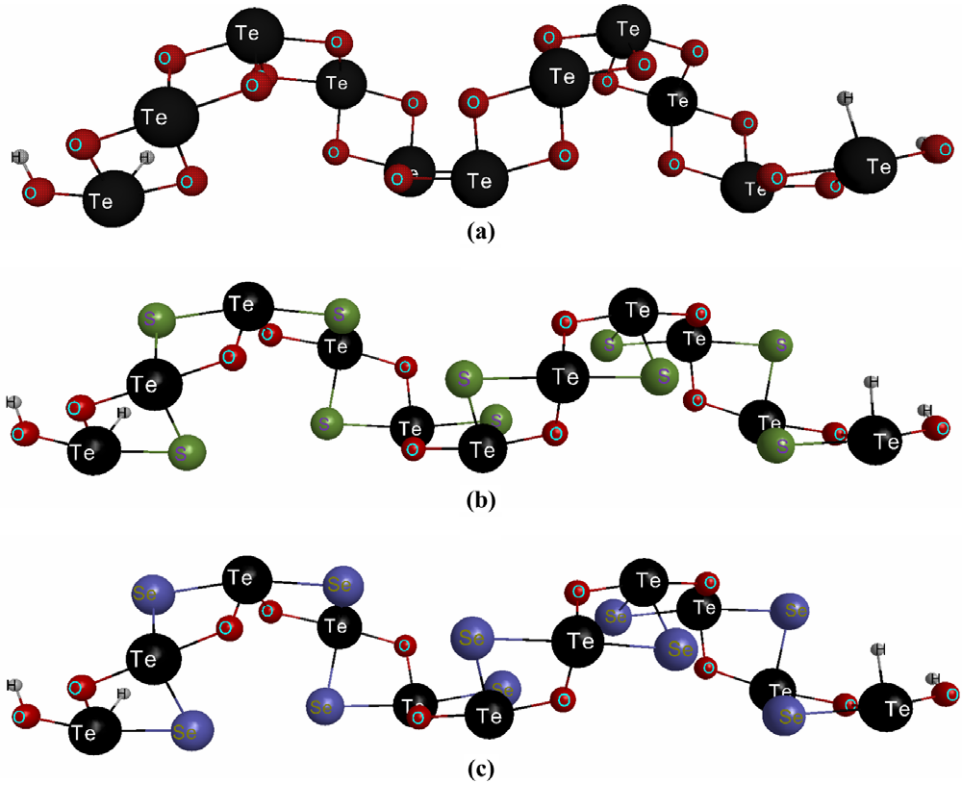

Figure 2. The helix-like 3D structure of the molecular cluster $(TeOX)_nTeO_2$ with structure $^{H-O}{}_H{>}Te{<}^O{}_X{>}Te{<}^X{}_O\cdots{}^O{}_X{>}$ $Te<{}^X{}_O{>}Te{<}^H{}_{O-H}$ and length corresponding to $n = 10$: (a) base tellurite glass chain (X = O); (b) mixed glass chain with sulfur substitution (X = S) and (c) with selenium substitution (X = Se). Hydrogen atoms are used to terminate the dangling bonds in order to preserve electrical neutrality of the molecular chain.

$^{-O}{}_{-O}{>}Te{<}^O{}_O{>}Te{<}^O{}_O\cdots{}^O{}_O{>}Te{<}^O{}_O{>}Te{<}^{O-}{}_{O-}$ with the result that TeO_4 units are 'linearly' connected one by one with edge sharing of two oxygen atoms at each connection. At both ends of a chain, one of the Te–O bonds is broken by modifiers to form TeO_3^+ (o-Te$<^O{}_O$), which represents a terminator with a dangling Te–O bond. In our computation, all the dangling bonds of a charged molecular structure of $^{-O}{}_{-}{>}Te{<}^O{}_O{>}Te\cdots Te{<}^O{}_O{>}Te{<}^-{}_{O-}$ are terminated by hydrogen atoms in order to preserve charge neutrality of $^{H-O}{}_H{>}Te{<}^O{}_O{>}Te{<}^O{}_O\cdots{}^O{}_O{>}Te{<}^O{}_O{>}Te{<}^H{}_{O-H}$. The chainlike structures of $^{H-O}{}_H{>}Te{<}^O{}_O{>}Te{<}^O{}_O\cdots{}^O{}_O{>}$ $Te{<}^O{}_O{>}Te{<}^H{}_{O-H}$, with a variable number (n) of basic units of TeO_2, are chosen as the base molecular clusters for our study. They can be represented more simply as $(TeO_2)_{n+1}$ $(=(TeOO)\times n+TeO_2)$. When the length (n) of this chain structure grows, the molecular assembly tends to spiral in order to reduce its energy, resulting in the helical 3D structure shown in figure 2(a).

In the mixed tellurite–chalcogenide glass, the vitreous network is still mainly constructed from bridges of partly covalent and partly ionic Te–O bonds. With the replacement of some of the oxygen atoms by sulfur or selenium in the molecular cluster, $^{H-O}{}_H{>}Te{<}^O{}_X{>}Te{<}^X{}_O\cdots{}^O{}_X{>}Te{<}^X{}_O{>}Te{<}^H{}_{O-H}$ with X = S (or Se), local Te–S (or Te–Se) bonds are created within the base TeO_2 molecular network. The molecular chains so created can be represented as $Te_{n+1}O_{n+2}S_n$ $(=(TeOS)_nTeO_2 = (TeOS)\times n + TeO_2)$ and $Te_{n+1}O_{n+2}Se_n$ $(=(TeOSe)_nTeO_2 = (TeOSe)\times n + TeO_2)$ for a ∼50% S and Se replacement, respectively. As shown in figures 2(b) and (c), their 3D structures corresponding to the minimum energy state are similar to that of the base tellurite chain. Because of the more polarizable Te–S (or Te–Se) covalent bonds along the zigzag path of Te–X–Te$\cdots$Te–X–Te, these mixed glasses should have a larger optical nonlinearity than the simple Te–O–Te$\cdots$Te–O–Te chains.

3. Approaches and simulation

For an instantaneous response to an incident electric field, the optical polarization can be expressed in a power series of the field strength [13, 26],

$$\vec{P} = \varepsilon_0 \overleftrightarrow{\chi}^{(1)} \cdot \vec{E} + \varepsilon_0 \overleftrightarrow{\chi}^{(3)} \cdot \vec{E} \otimes \vec{E} \otimes \vec{E} \qquad (1)$$

where the vector $\vec{P}$ is the macroscopic polarization and the vector $\vec{E}$ the externally applied electric field. $\overleftrightarrow{\chi}^{(m)}$, the mth-order nonlinear optical susceptibility, is the $(m+1)$th-rank tensor that represents the strength of the mth-order nonlinear process. The operator $\otimes$ denotes the tensor product and ε_0 is the permittivity of vacuum. The material is actually composed of a finite number of molecular clusters, each with a molecular dipole moment polarized by the localized electric field $\vec{E}_{\rm loc}$. A corresponding expression for the microscopic dipole $\vec{p}$ is

$$\vec{p} = \varepsilon_0 \overleftrightarrow{\alpha} \cdot \vec{E}_{\rm loc} + \varepsilon_0 \overleftrightarrow{\gamma} \cdot \vec{E}_{\rm loc} \otimes \vec{E}_{\rm loc} \otimes \vec{E}_{\rm loc} \qquad (2)$$

where the second-rank tensor $\overleftrightarrow{\alpha}$ and the fourth-rank tensor $\overleftrightarrow{\gamma}$ are referred to as the microscopic linear polarizability and second hyper-polarizability (or third-order polarizability), corresponding to the linear and third-order nonlinear processes respectively. Using the Lorentz approximation, the local field $\vec{E}_{\text{loc}}$ can be expressed in terms of the externally applied field and the induced polarization as

$$\vec{E}_{\text{loc}} = \vec{E} + L \cdot \vec{P} = f \cdot \vec{E} \tag{3}$$

where L (or f) is the so-called local field (or Lorentz–Lorenz) factor and $L = \frac{1}{3\varepsilon_0}$ (or $f = \frac{\chi^{(1)}}{3} + 1$) [13, 26, 27].

In our *ab initio* quantum mechanical approach, we assume that the electron wavefunction in a molecular cluster is well approximated by a linear combination of atomic orbitals (LCAO-MO) [9–12]. The computations have been performed with the quantum chemistry program package GAMESS [8] using the density functional theory (DFT) [12]. A hybrid exchange–correlation function of the Becke, three-parameter, Lee–Yang–Parr (B3LYP) [12] type is employed to construct a linear combination of Hartree–Fock and other correlated functions. The basis valence set proposed by Stevens, Basch, Krauss, Jasien and Cundari (SBKJC) [28] with an augmentation of both the diffuse *sp* and polarization 3*d* functions [19] was chosen in the effective core potential (ECP). A HONDO/Rys type integral was used for all integral derivatives within the self-consistent field (SCF) approximation and the convergence criterion was chosen to be 10^{-10}. The geometries of the molecular structures were first determined by minimizing their energies. The gradient tolerance was set to 10^{-10} in search of a geometry convergence. After this minimization, molecular chain structures of various lengths (greater than 5 units) were all found to assume the helical shape shown in figure 2. Shorter chains could not complete a period of the helical structure. The microscopic linear polarizability ($\overleftrightarrow{\alpha}$) and second hyper-polarizability ($\overleftrightarrow{\gamma}$) of the molecular chains were then computed based on these optimized geometries using the finite field method [8], by evaluating the electronic contribution to the molecular dipole moment in the presence of a static field. This procedure gives off-resonant hyper-polarizabilities that are valid in the infrared spectral range far away from one- and two-photon resonances. Such hyper-polarizability values are most interesting because they make it possible to better compare different materials, and because for the materials we are studying they directly give third-order susceptibilities that are appropriate for describing nonlinear optical interactions near 1.5 μm and at longer wavelengths in the infrared spectral region.

In GAMESS, the reference axes are chosen to be the principal optical ones so that the tensor $\overleftrightarrow{\alpha}$ is diagonal. However, as the chain length grows, these references axes vary and they do not necessary align with the main rotational axis of the cylindrical helix. It is then meaningless to compare the magnitude of individual elements of the tensors $\overleftrightarrow{\alpha}$ and $\overleftrightarrow{\gamma}$. In the following, we will therefore use the scalar polarizabilities obtained by rotationally averaging the full tensor,

$$\alpha_{\text{av}} = (\alpha_{xx} + \alpha_{yy} + \alpha_{zz})/3 \tag{4}$$

$$\gamma_{\text{av}} = (\gamma_{xxxx} + \gamma_{yyyy} + \gamma_{zzzz} + 2\gamma_{xxyy} + 2\gamma_{yyzz} + 2\gamma_{zzxx})/5 \tag{5}$$

where α_{xx}, α_{yy} and α_{zz} are the microscopic linear polarizabilities for an electric field along the x, y and z directions, and γ_{xxxx}, γ_{yyyy}, γ_{zzzz}, γ_{xxyy} ($=\gamma_{yyxx}$), γ_{yyzz} ($=\gamma_{zzyy}$) and γ_{zzxx} ($=\gamma_{xxzz}$) are the elements of the fourth-rank tensor of $\overleftrightarrow{\gamma}$. Using these rotational averages gives us a much better insight into how the polarizability changes with increasing chain length and provides results that are particularly well adapted to a randomly oriented glass assembly.

As mentioned earlier, the molecular structures investigated computationally were constructed with a variable number (n) of TeOX units (X = O, S or Se) introduced in the base TeO_2 glass. In general, the hyper-polarizabilities of molecular chains increase with length. To analyze the length dependence, it is important to distinguish the incremental contribution of a single TeOX unit from the properties of the whole chain. Below, we will show that the chain length dependence of linear and nonlinear polarizabilities can be very well described by

$$\alpha_{\text{av}} = \alpha_0 + \alpha_1 \cdot n \tag{6}$$

$$\gamma_{\text{av}} = \gamma_0 + \gamma_1 \cdot n^r \tag{7}$$

where the rotationally averaged linear polarizability α_0 and second hyper-polarizability γ_0 due to the basis TeO_2 are always taken as an offset so that the second terms can then be considered as the effect from incremental units of $(TeOX)_n$. In that case, the slope α_1 simply represents the net (linear) gain of linear polarizability from a single additional unit of TeOX. As the length n grows, the enhancement of the second hyper-polarizability is more strongly influenced (nonlinear) due to the exponent r.

At the macroscopic level, the polarizability of a material is directly taken as the sum effect of the microscopic dipoles of all the molecular clusters [13, 26]

$$\chi^{(1)} = N \cdot f \cdot \alpha_{\text{av}} \tag{8}$$

$$\chi^{(3)} = N \cdot f^4 \cdot \gamma_{\text{av}} \tag{9}$$

where N is the number density of molecular chains and the factor f represents the local field effect mentioned earlier. The first-order susceptibility $\chi^{(1)}$ is related to the linear refractive index n_0 by $\chi^{(1)} = n_0^2 - 1$.

4. Results and discussion

Ab initio numerical computations were performed to obtain the linear polarizability, $\overleftrightarrow{\alpha}$, and second hyper-polarizability, $\overleftrightarrow{\gamma}$, for molecular chains $(TeOX)_nTeO_2$ (X = O, S or Se) of varying lengths from $n = 1$ to 10. As mentioned before, the molecular chains assumed the helix-like structures shown in figure 2 in their minimum energy configuration. The calculated results for both base and mixed glasses are plotted in figure 3 as rotationally averaged $\overleftrightarrow{\alpha}$ and $\overleftrightarrow{\gamma}$ versus molecular length for $n = 1$–10.

The clear linear trends observed for α_{av} suggest a constant polarizability per unit length. This indicates that

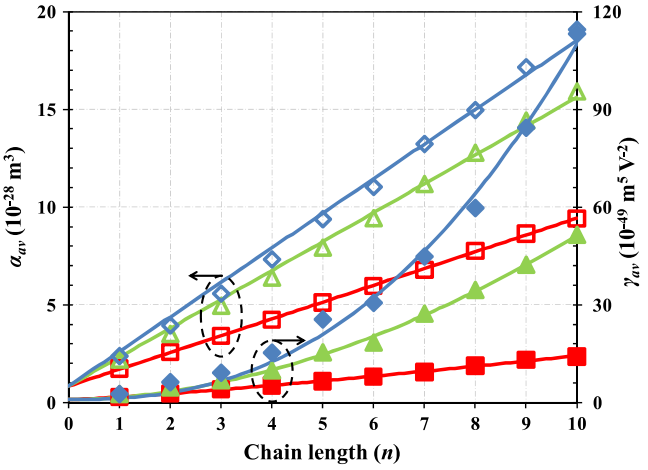

Figure 3. α_{av} and γ_{av} plotted for varying chain lengths n of the molecular cluster $(TeOX)_nTeO_2$ with structure $^{H-O}{}_{H}>Te<^{O}{}_{X}>Te<^{X}{}_{O}\cdots{}^{O}{}_{X}>Te<^{X}{}_{O}>Te<^{H}{}_{O-H}$. α (in the unit of 10^{-28} m^3, □ X = O with a linear fitting of $\alpha_{av} = 0.84 + 0.86n$, △ X = S with a linear fitting of $\alpha_{av} = 0.84 + 1.48n$, and ◊ X = Se with a linear fitting of $\alpha_{av} = 0.84 + 1.77n$) and γ (in units of 10^{-49} m^5 V^{-2}, ■ X = O with an exponential fitting of $\gamma_{av} = 0.91 + 0.79n^{1.23\pm0.27}$, ▲ X = S with an exponential fitting of $\gamma_{av} = 0.91 + 0.69n^{1.87\pm0.11}$, and ♦ X = Se with an exponential fitting of $\gamma_{av} = 0.91 + 0.39n^{2.44\pm0.07}$).

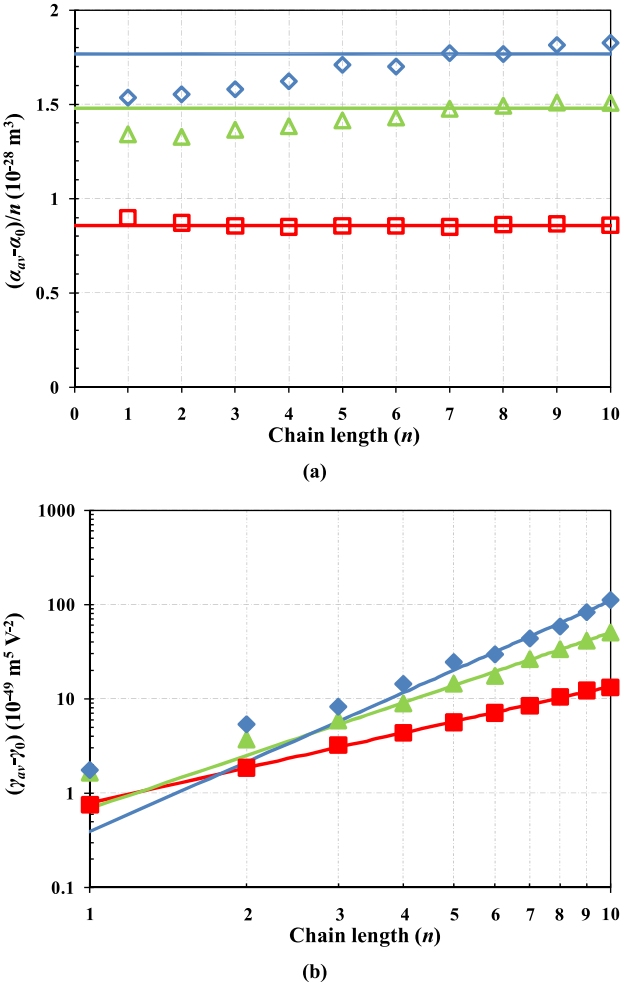

Figure 4. (a) Averaged linear polarizability $(\alpha_{av} - \alpha_0)/n = \alpha_1$ and (b) second hyper-polarizability $(\gamma_{av} - \gamma_0)$ plotted for variable chain lengths n of the molecular chains $(TeOX)_nTeO_2$ with structure $^{H-O}{}_{H}>Te<^{O}{}_{X}>Te<^{X}{}_{O}\cdots{}^{O}{}_{X}>Te<^{X}{}_{O}>Te<^{H}{}_{O-H}$ based on our *ab initio* computational results. α is on a linear scale (□ X = O, △ X = S and ◊ X = Se) and γ is on a logarithmic scale (■ X = O, ▲ X = S and ♦ X = Se).

the linear polarizability of the full helix-like linear chain of $(TeOX)_nTeO_2$ is the same as that which would be obtained from a number (n) of unconnected units of TeOX embedded in the TeO_2 network. We fit the data with a linear function $\alpha_{av} = \alpha_0 + \alpha_1 \cdot n$, which has the same intercept α_0 for all molecular chains because they all have the same basis of TeO_2. The slope α_1 reveals the linear polarizability contribution of each separate TeOX unit. It increases from 0.86×10^{-28} to 1.77×10^{-28} m^3 when X goes from the lightest atom O to the heaviest atom Se, as shown in figure 4(a).

In contrast, a nonlinear enhancement is observed for the rotationally averaged second hyper-polarizability with increasing chain length. We fit the result from the quantum chemical computation using a power law $\gamma_{av} = \gamma_0 + \gamma_1 \cdot n^r$ with a common offset γ_0 for all glasses. The length dependence of the third-order polarizability given in figure 3 is described by an exponent r greater than unity for all three kinds of glasses. As the chain length increases, γ_{av} increases faster than for a simple concatenation of individual TeOX units. The replacement of oxygen by chalcogen boosts the r values from 1.23 to 1.87 and as high as 2.44, for S and Se respectively, corresponding to the oblique lines shown in figure 4(b). It should be noted that this exponent remains much smaller than that typical of conjugated chains of carbon atoms, where the delocalization effect of the electron over a molecular chain caused by π-bonds is much stronger [29].

It is also important to note that the proposed molecular chains only reach a fully developed helical shape for $n \geqslant 4$, which accounts for the deviation from the general trend for shorter lengths. A good agreement between the data points and the trends for both α_{av} and γ_{av} is observed for longer molecules. The important point here is that a clear upshift in α_1 and r is observed as a result of the replacement of O by S and Se. This can be understood from the simple fact that both the linear and the nonlinear polarizabilities grow with the size of the electronic wavefunctions and the overlap between the highest occupied molecular orbital (HOMO) and the lowest unoccupied molecular orbital (LUMO), and decrease with increasing energy separation between the ground state and the first optically accessible excited state [13]. For the glasses that we are studying, the sizes of the electronic wavefunctions are mainly determined by the bond length between Te and O, Te and S or Te and Se. Table 1 gives the bond lengths and excitation energies for these structures and shows that the higher nonlinearities directly correlate with the lower excitation energies and longer bond lengths of the Te–S and the Te–Se bonds when compared to the Te–O bond.

In the following, we discuss how the microscopic polarizabilities we determined can be used to estimate the macroscopic optical and nonlinear optical properties of a glass. If a bulk glass is synthesized from these proposed molecular

Table 1. Bond lengths and excitation energies obtained in our GAMESS computation.

Molecular chain	Bond length (Å)		Excitation energy (eV)
	Short bond	Long bond	
$(TeOO)_nTeO_2$	Te–O ∼ 1.90[a] (∼1.88[b])	Te–O ∼ 2.10[a] (∼2.12[b])	∼3.00[c]
$(TeOS)_nTeO_2$	Te–S ∼ 2.40[a] (∼2.47[b])	Te–S ∼ 2.66[a] (∼2.69[b])	∼2.05[c]
$(TeOSe)_nTeO_2$	Te–Se ∼ 2.55[a] (∼2.60[b])	Te–Se ∼ 2.80[a] (∼2.60[b])	∼1.67[c]

[a] Values computed in this work.

[b] Typical experimental bond lengths reported in the literature [36–38].

[c] The excitation energy of a molecular chain $(TeOO)_nTeO_2$ ($n = 2$) as calculated in GAMESS has been scaled by a factor of 2 to match the experimental band gap for pure tellurite glasses [3]. The same factor was then used to correct the calculated value of $(TeOS)_nTeO_2$ and $(TeOSe)_nTeO_2$.

chains of n units, its macroscopic susceptibilities $\chi^{(1)}$ and $\chi^{(3)}$ will depend upon how many chains are 'packed' into a unit volume. We therefore need to estimate the molecular number density (number of molecules per unit volume) as the size of the molecules grows and for glasses of different compositions. The molecular size may be tracked by counting the number of atoms within a molecular chain and assigning the same volume to each atom. For pure tellurite glass, we assign the number density of TeO_2 units at $n = 0$ to the number density value 2.1×10^{28} m^{-3} reported in the literature [30, 31]. Considering a molecular chain with length n as a new unit, it is necessary to rescale the number density accordingly. Therefore, as the size of a pure tellurite molecular chain grows to $n = 10$, the number density is correspondingly reduced 11-fold, to 1.9×10^{27} m^{-3}. Using this reduction factor and using the relative size differences between O, S, and Se, we estimate the number density corresponding to $n = 10$ to be 1.5×10^{27} m^{-3} for X = S and 1.3×10^{27} m^{-3} for X = Se. Then, we use equations (8) and (9) to convert from the microscopic linear polarizability α_{av} and second hyper-polarizability γ_{av} to the macroscopic linear susceptibility $\chi^{(1)}$ (or the linear refractive index n_0) and third-order susceptibility $\chi^{(3)}$, respectively. This procedure approximates the structure of the macroscopic glass by a dense assembly or randomly oriented, identical molecular units. We compared the linear and third-order susceptibilities obtained in this way to the experimental values for pure tellurite glass and found a good agreement. The actual experimental values for pure tellurite are obtained when multiplying the computed α_{av} by a factor of 0.85 and the computed γ_{av} by a factor of 0.3, respectively. The reason for the discrepancy described by these correction factors can be found both in the ability of our *ab initio* calculations to predict the actual absolute values of the polarizabilities and in the way we estimate the macroscopic susceptibilities, including the use of the Lorentz local field corrections. In any case, we have chosen to use the same factors that we found for pure tellurite to correct the computed polarizability values for mixed glasses. This has the advantage that we can show our result on an absolute scale, directly relating numerical values to the experimental ones of pure tellurite glasses. The final results are shown in figure 5. These results predict the linear (a) and third-order nonlinear (b) optical susceptibilities of glasses made of mixed tellurite–chalcogenide molecular chains with a helical structure, and reveal how these susceptibilities grow with the length of the substituted chains. These results are also compared with those for pure tellurite molecular chains of the same length. Because of the nonlinearity introduced by the local field correction factors, the fluctuations in the predicted macroscopic susceptibilities with increasing chain length are larger when plotting macroscopic polarizabilities than when plotting molecular hyper-polarizabilities.

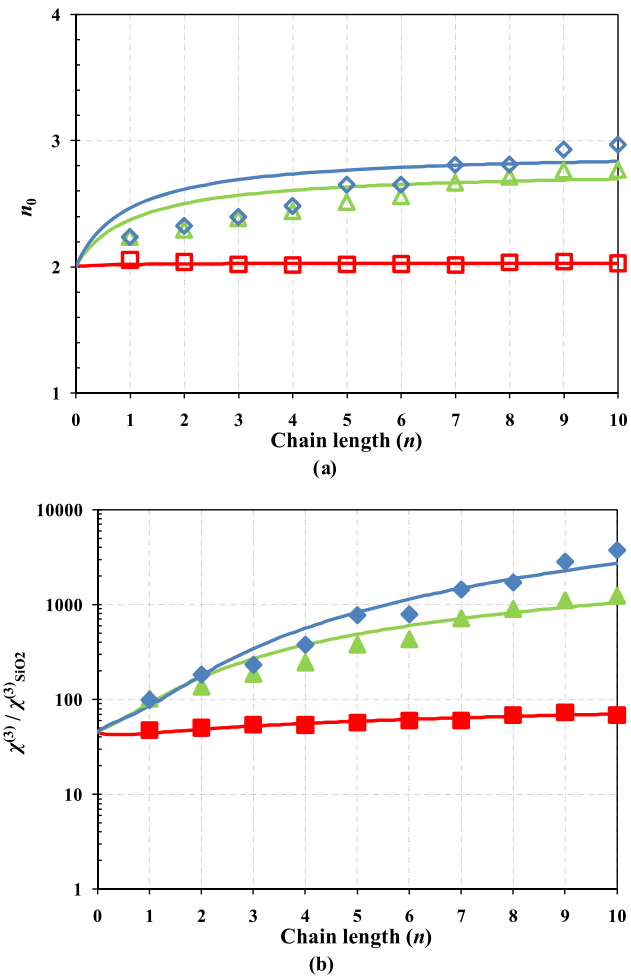

Figure 5. The macroscopic refractive index and third-order susceptibility for glasses composed of molecular chains $(TeOX)_nTeO_2$ with structure $^{H-O}{}_{H}{>}Te{<}^{O}{}_{X}{>}Te{<}^{X}{}_{O}\cdots{}^{O}{}_{X}{>}Te{<}^{X}{}_{O}{>}Te{<}^{H}{}_{O-H}$ obtained from *ab initio* calculations. The third-order susceptibilities, $\chi^{(3)}$, are normalized to the value of fused silica. n_0 (□ X = O, △ X = S and ◇ X = Se) and $\chi^{(3)}$ (■ X = O, ▲ X = S and ♦ X = Se).

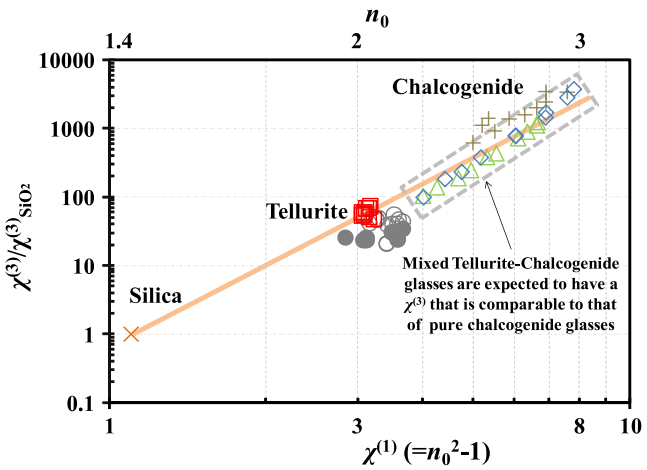

Figure 6. $\chi^{(3)}$ versus $\chi^{(1)}$ plotted on a logarithmic scale for fused silica (× literature data [32]), tellurite glasses (○ literature data [30, 31, 33] and ● experimental data measured by us) and chalcogenide glasses (+ literature data [34]). $\chi^{(3)}$ susceptibilities of the base tellurite glasses (□ X = O) and mixed tellurite–chalcogenide glasses (△ X = S and ◇ X = Se) are estimated assuming that each glass is made up of a fixed number of units n from 1 to 10. The linear and nonlinear optical properties of mixed glasses can cover a broad range indicated by the dashed box. All $\chi^{(3)}$ values are normalized to that of fused silica for convenient comparison.

The linear and nonlinear optical properties predicted using the above procedure match very well the global trend observed in these glasses in general. A general intrinsic relation between macroscopic third-order optical nonlinear susceptibility $\chi^{(3)}(-\omega;\omega,\omega,-\omega)$ and linear susceptibility $\chi^{(1)}(-\omega;\omega)$ at the optical frequency ω for solids with similar density to our glasses is known to exist, that follows the empirical Miller's rule extended to the case of third-order nonlinear optics and predicts a constant ratio of $\chi^{(3)}/[\chi^{(1)}]^4$ [13]. As shown in figure 6, the three main families of glasses, silica (× [32]), tellurite (○ [30, 31, 33] and ●) and chalcogenide (+ [34]), indeed follow this trend, which is represented by a straight line in the logarithmic plot. If the mixed glass we suggest can be successfully synthesized, the molecules formed inside will most likely contain chains of different lengths, with macroscopic properties that will depend on the statistical distribution of these chain lengths, which in turn will depend on the glass constituents and on their relative concentrations. Different values of chain lengths n could then also be translated into corresponding fractions of the glass made of mixed TeOX units. In figure 6 we have plotted our results for all values of n to give an idea of the range of values that could be expected in a mixed glass. The data cover a broad range of $\chi^{(1)}$ and $\chi^{(3)}$, indicated in figure 6 by the dashed box with the symbols of △ (X = S) and ◇ (X = Se) inside, from $\chi^{(1)} = \sim 4$ and $\chi^{(3)}/\chi^{(3)}_{SiO_2} = \sim 100$ to $\chi^{(1)} = \sim 8$ and $\chi^{(3)}/\chi^{(3)}_{SiO_2} = \sim 4000$ as the length varies from $n = 1$ to 10. In comparison, for the base tellurite glasses indicated by the symbol □ (X = O), we do not observe a strong enhancement of the third-order polarizability for pure $(TeOO)_nTeO_2$ with longer chain lengths, indicating that the nonlinearity of the base glass is essentially localized on a tellurium–oxygen bond. Our calculations therefore follow the trend predicted by Miller's rule extended for third-order nonlinear optics, and they show that introducing chalcogen elements significantly enhances the nonlinearity of the base tellurite glass, raising the linear and nonlinear optical susceptibilities well into the chalcogenide region, even for intermediate lengths (corresponding to chains with $n \approx 5$).

5. Conclusions

Chalcogen-modified tellurite glasses $^{H-O}{}_{H}{>}Te{<}^{O}{}_{X}{>}Te{<}^{X}{}_{O}\cdots{}^{O}{}_{X}{>}Te{<}^{X}{}_{O}{>}Te{<}^{H}{}_{O-H}$ partially substituted with X = S or Se have been analyzed with respect to their functional optical and nonlinear optical properties, and compared with the base tellurite glass (X = O). The effect of this substitution on the refractive index and the third-order optical nonlinearity of the glass has been studied through *ab initio* quantum chemistry calculations. Our results indicate that $(TeOX)_nTeO_2$ chains assume a helical shape and that introducing chalcogen into the base tellurite glass can enhance $\chi^{(3)}$ up to ∼40 times that of the base glass (the largest enhancement would correspond to the case of Se substitution for the longest calculated chain with $n = 10$). With fewer than half the oxygens replaced by chalcogen atoms, the nonlinear optical performance of these mixed glasses would be comparable with that of chalcogenides, with better chemical stability and lower photosensitivity.

Acknowledgments

This work was supported by a grant from the National Science Foundation, DMR-0701526 'Glass science, processing and optical properties of tellurite fibers'.

References

[1] Eason R W and Miller A (ed) 1993 *Nonlinear Optics in Signal Processing* (London: Chapman and Hall)
[2] Alfano R R (ed) 2005 *The Supercontinuum Laser Source: Fundamentals with Updated References* (New York: Springer)
[3] El-Mallawany R A H 2001 *Tellurite Glasses Handbook: Physical Properties and Data* (Boca Raton, FL: CRC Press)
[4] Zakery A and Elliott S R 2007 *Optical Nonlinearities in Chalcogenide Glasses and their Applications* (Berlin: Springer)
[5] Zuckerman J J and Hagen A P (ed) 1991 *Inorganic Reactions and Methods* (*The Formation of Bonds to Group VIB (O, S, Se, Te, Po) Elements (Part 1)* vol 5) (New York: Wiley–VCH)
[6] Devillanova F A 2006 *Handbook of Chalcogen Chemistry: New Perspectives in Sulfur, Selenium and Tellurium* (Cambridge: Royal Society of Chemistry)
[7] Jin Z, Zhang A, Kovalskiy A, Biaggio I and Toulouse J 2009 *Conf. on Lasers and Electro-Optics/Int. Quantum Electronics Conf.* Optical Society of America p JWA25
[8] Schmidt M W *et al* 1993 *J. Comput. Chem.* **14** 1347
[9] Simons J 2003 *An Introduction to Theoretical Chemistry* (Cambridge: Cambridge University Press)
[10] Lowe J P 2005 *Quantum Chemistry* (Amsterdam: Academic)

[11] Levine I N 2008 *Quantum Chemistry* (Upper Saddle River, NJ: Prentice-Hall)
[12] Jensen F 2006 *Introduction to Computational Chemistry* (Chichester: Wiley)
[13] Boyd R W 2003 *Nonlinear Optics* (Amsterdam: Academic)
[14] Mirgorodsky A P, Soulis M, Thomas P, Merle-Mejean T and Smirnov M 2006 *Phys. Rev.* B **73** 134206
[15] Soulis M, Merle-Méjean T, Mirgorodsky A P, Masson O, Orhan E, Thomas P and Smirnov M B 2008 *J. Non-Cryst. Solids* **354** 199
[16] Suehara S, Yamamoto K, Hishita S, Aizawa T, Inoue S and Nukui A 1995 *Phys. Rev.* B **51** 14919
[17] Suehara S, Hishita S, Inoue S and Nukui A 1998 *Phys. Rev.* B **58** 14124
[18] Champarnaud-Mesjard J C, Blanchandin S, Thomas P, Mirgorodsky A, Merle-Méjean T and Frit B 2000 *J. Phys. Chem. Solids* **61** 1499
[19] Suehara S *et al* 2004 *Phys. Rev.* B **70** 205121
[20] Ceriotti M, Pietrucci F and Bernasconi M 2006 *Phys. Rev.* B **73** 104304
[21] Thomas P A 1988 *J. Phys. C: Solid State Phys.* **21** 4611
[22] Beyer V H 1967 *Z. Kristallogr.* **124** 228
[23] Sekiya T, Mochida N and Ohtsuka A 1994 *J. Non-Cryst. Solids* **168** 106
[24] Sakida S, Hayakawa S and Yoko T 1999 *J. Non-Cryst. Solids* **243** 1
[25] Sakida S, Hayakawa S and Yoko T 1999 *J. Non-Cryst. Solids* **243** 13
[26] Shen Y R 2002 *The Principles of Nonlinear Optics* (Hoboken, NJ: Wiley–Interscience)
[27] Kittel C 2004 *Introduction to Solid State Physics* (New York: Wiley)
[28] Stevens W J, Basch H and Krauss M 1984 *J. Chem. Phys.* **81** 6026
[29] Slepkov A D, Hegmann F A, Eisler S, Elliott E and Tykwinski R R 2004 *J. Chem. Phys.* **120** 6807
[30] Yousef E, Hotzel M and Russel C 2004 *J. Non-Cryst. Solids* **342** 82
[31] Yousef E, Hotzel M and Russel C 2007 *J. Non-Cryst. Solids* **353** 333
[32] Milam D 1998 *Appl. Opt.* **37** 546
[33] Souza R F, Alencar M A R C, Hickmann J M, Kobayashi R and Kassab L R P 2006 *Appl. Phys. Lett.* **89** 171917
[34] Harbold J M, Ilday F Ö, Wise F W, Sanghera J S, Nguyen V Q, Shaw L B and Aggarwal I D 2002 *Opt. Lett.* **27** 119
[35] Bode B M and Gordon M S 1998 *J. Mol. Graph. Modelling* **16** 133
[36] Suehara S, Konishi T and Inoue S 2006 *Phys. Rev.* B **73** 092203
[37] Foss O 1962 *Acta Chem. Scand.* **16** 779
[38] Afify N, Gaber A, Abdalla I and Talaat H 1997 *Physica* B **229** 167